Spring 2022

Characterization of Carbon Fiber PEKK Thermoplastic Prepreg for Process Modeling

Tanner M. Leo

CHARACTERIZATION OF CARBON FIBER PEKK THERMOPLASTIC PREPREG FOR PROCESS MODELING

Tanner M. Leo
Western Washington University
Bellingham, WA, 98225

ABSTRACT

Thermoplastic composites are of rapidly growing interest to the aerospace industry due to their potential to save energy through processing or material through recycling or repair. Process modeling is a computational-based approach for predicting material behavior and quality outcomes for different manufacturing processes. In effect, process modeling reduces both the risk and cost associated with manufacturing composite parts. Process modeling of thermoplastic composites is largely still ill-defined, although a model structure has been defined and validated with carbon fiber poly(ether ether ketone) (CF/PEEK) composite prepreg. Carbon fiber poly(ether ketone ketone) (CF/PEKK) was subjected to a series of characterization experiments CF/PEKK and neat PEKK samples were characterized by modulated differential scanning calorimetry (MDSC), dynamic mechanical analysis (DMA), rheology, and guarded heat flow metrology. Data were analyzed and prepared for building the constitutive models for crystallization and melting kinetics, specific heat capacity, stress relaxation, modulus development, flow characteristics, thermal conductivity, coefficient of thermal expansion, and density. Challenges associated with carrying out a full suite of characterization experiments were identified and the material behavior observed for CF/PEKK was described, providing a framework for characterizing high-performance thermoplastic prepreg for process modeling.

1. INTRODUCTION

Developing new composite processes can be an expensive and high-risk process, especially with novel and unproven designs, and unfamiliar materials. There is a wide range of processing outcomes that all affect the mechanical and physical properties of a part and its overall performance. These include different thermal outcomes (such as degree of crystallinity or degree of cure), quality-based outcomes (such as voids, fiber/resin ratio, and wrinkling of plies), and mechanical outcomes (such as residual stresses and dimensional changes) [1]. Optimizing the processing parameters to achieve the desired quality outcome typically requires designed experiments with the processing parameters as factors. These experiments can be prohibitively expensive for smaller companies. It is therefore a shared interest of the composite engineering industry to develop methods and tools to reduce the initial investment cost of developing new composite processes.

Process modeling, sometimes called process simulation, is a computation-based approach used to predict processing outcomes for a given manufacturing process. The merit of process modeling is in the cost-reducing potential. Parts need not be produced to evaluate whether the processing parameters were successful in reaching the design criteria. Rather, only a few small testing

specimens need to be produced and then characterized, to build a predictive model capable of determining the process outcomes for larger parts. To date, there have been numerous models proposed in the literature for thermosetting composites, able to predictively explain the different phenomena of material's behavior from the micro-scale to macro-scale.

While it is not the case for thermosetting prepreg, process modeling of thermoplastic prepreg is ill-defined. There is ambiguity both in the specifics of the experiments used to characterize the desired properties, as well as the methods to be used to validate the results and test the accuracy of the model predictions. Currently, in the literature, there is only one thermoplastic prepreg material for which a complete set of constitutive models has been proposed: carbon fiber and poly(ether ether ketone) (CF/PEEK) [2]. This model has only been applied to one other thermoplastic prepreg material in a quasi-empirical way [3].

The use of composites in the transportation sector has grown tremendously over the past decade. The aerospace industry, in particular, is necessitating the use of lighter and stronger composite materials, with the Advisory Council for Aviation Research and innovation in Europe (ACARE) aiming to reduce the CO_2 emissions per passenger kilometer by 75% from 2000 [4]. While there is growing interest in the aerospace industry for thermoplastic composite prepreg materials, these materials are not new to the industry. Thermoplastics were first used on structural aircraft components in 1980 when the US military used thermoplastics in the landing gear and weapons-bay doors of the F-22 fighter jet. The reason that thermoplastic composites use is not widespread in the aerospace industry is not due to the mechanical performance or feasibility of the parts, but simply due to the cost and difficulty of manufacturing [4].

Today, there are new incentives for the aerospace industry to shift away from thermosetting composites and toward thermoplastic composites. Thermosetting composites are traditionally processed in an autoclave, which is recognized as an outdated process and a bottleneck to new innovative processing techniques. Due to the nature of the molecular structure, thermoplastic composites have the potential to be manufacturing using more efficient methods such as laser-assisted automated-tape-laying (LATL) [5]. Other benefits such as recyclability, and energy savings during storage serve as additional incentives. Further developing process modeling capabilities for thermoplastic prepreg will both aid the development of novel and more efficient processing techniques, but will also make the adoption of thermoplastic composites in industries such as aerospace a much simpler task.

1.1 Purpose

This paper will describe a potential approach to characterizing a thermoplastic prepreg material to build a full set of constitutive models for process simulation. This paper will not attempt to document the process of fitting the collected data to the appropriate equations, nor will it provide a case study to evaluate the predictive accuracy of the model produced. This paper provides researchers with a framework for conducting the necessary characterization experiments, while also contending with the necessary considerations and factors influencing the choice of experimental methods.

2. EXPERIMENTATION

Solvay APC carbon fiber poly(ether ketone ketone) (CF/PEKK) unidirectional tape, a 70/30 grade of PEKK was used to prepare samples for thermal conductivity, CTE, DSC, and DMA samples. Fourteen plies measuring 4" by 8" were arranged and compression-molded at 350 °C for 20 minutes, with about 1 ton of force applied. The laminate was cooled in the press with pressure still applied. For the thermal conductivity, coefficient of thermal expansion, modulus development, and stress relaxation experiments, samples were cut from the laminate with a diamond hole saw or tile saw. Rheology samples of unreinforced PEKK were prepared using a PIKE Technologies 13 mm Evacuable Pellet Press die and a hot press. Powdered resin weighing 2.15 g was held at 350 °C under a 0.1-ton force for 30 minutes.

A TA Instruments Q100 DSC was used for the crystallization and melting kinetics, isothermal crystallization, isothermal degradation, and specific heat capacity experiments. All DSC experiments used standard pans with masses less than 0.05 mg of each other, 5 mg samples, and an inert atmosphere. Quasi-isothermal degradation experiments were used to determine an upper processing temperature of other experiments, by looking at trends in reversible heat capacity, finding 375 °C to be optimal. Crystallization and melting kinetics were studied using modulated non-isothermal heat-only experiments with 7 ramp rates between 1 °C/min and 13 °C/min, two replicates per ramp rate, three heat-cool cycles per experiment, a temperature range between 25 °C and 375 °C with the third cycle conducted at 400 °C, and a 5-minute isothermal hold at temperature. Isothermal crystallization experiments were conducted at 7 temperatures between 300 °C and 315 °C. Heat capacity experiments were conducted on unreinforced PEKK and a 26.4 mg sapphire reference sample and utilized a 2 °C/min heat-cool with a 15-minute isothermal hold at temperature. Modulation parameters included a period of 100 s and an amplitude of ± 1 °C.

A TA Instruments Q800 DMA with a 50 mm span 3-pt bending fixture was used for modulus development and stress relaxation experiments. DMA samples had approximate dimensions of 55 mm by 12 mm by 2 mm, and standard parameters included a static force of 0.01 N and 0.1% strain. Modulus development experiments utilized a 15-minute soak at 40 °C followed by a 2 °C/min ramp to 280 °C, and a frequency of 0.1 Hz. Stress relaxation experiments were conducted at temperatures between 30 °C and 320 °C at increments of 10 °C, where a strain was held for 10 minutes at a constant temperature, and stress was measured. Three replicates were used for both experiments.

A TA Instruments DHR-2 stress-controlled rheometer was used to determine CTE and characterize viscosity. Both experiments used 25 mm parallel aluminum plates, three replicates, and a 2 °C/min ramp rate. CTE measurements utilized a 25 mm diameter CF/PEKK sample, while viscosity measurements used a 13 mm PEKK pellet that was melt pressed to 25 mm diameter and 1 mm thickness. The CTE experiment consisted of a heat-cool cycle between 50 °C to 250 °C, with a constant axial force of 0.5 N ± 0.1 N. Viscosity measurements consisted of a cool-heat cycle between 375 °C and 150 °C, with 0.1 % strain and 1 Hz frequency.

Thermal conductivity was measured with a Thermtest GHFM-01. Samples of CF/PEKK were 2 mm thick and 50.1 mm in diameter. Instrument calibrations were performed on three standard materials: Pyrex, stainless steel, and titanium. All measurements were conducted at temperatures between 50 °C and 210 °C at increments of 20 °C, with a temperature gradient of ± 10 °C. Density was measured using a density determination kit and analytical balance. The temperature of the

ambient air and ultrasonicated water were noted for calculations, and the measurement was performed twice for replicability.

3. RESULTS

3.1 Crystallization & Melting Kinetics

CF/PEKK was subjected to non-isothermal modulated differential scanning calorimetry experiments. Crystallization, cold crystallization, and melting transitions were analyzed for ramp rates of 1 °C/min, 2 °C/min, 4 °C/min, 7 °C/min, 9 °C/min, 11 °C/min, and 13 °C/min, with two samples used for each ramp rate to assess replicability. The non-reversing heat flow signal was used for the analysis of crystallization and cold crystallization events. Melting transitions were examined using both the reversing and non-reversing heat flow signals. Heat flow signals were passed through a Savitzky–Golay filter before drawing baselines and calculating crystallinity [6].

Baselines were drawn for the transitions using an adaptive baseline technique. First, two temperature endpoints were selected manually on either side of the transition. A linear regression calculation was performed on a user-defined number of heat flow data points to either side of the selected endpoints. The parameters for these regressions were selected to best represent the slope on either side of the transition. A linear baseline was drawn between the two points, and conversion α of crystallization was calculated as a function of temperature and time by integrating the heat flow curve with the linear baseline subtracted. Next, an adaptive baseline was drawn using the equation:

$$\mathrm{AB(T)} = \left(\mathrm{m_{T1}} \cdot \alpha(\mathrm{T}) + \mathrm{m_{T2}}\left(1 - \alpha(\mathrm{T})\right)\right) \cdot \mathrm{T} + \left(\mathrm{b_{T1}} \cdot \alpha(\mathrm{T}) + \mathrm{b_{T2}}\left(1 - \alpha(\mathrm{T})\right)\right) \quad (1)$$

Where m_{T1} and m_{T2} are the slopes at the temperatures $T1$ and $T2$, and b_{T1} and b_{T2} are the intercepts of the linear equations regressed on the data near those temperatures. Conversion α was calculated again, with the original heat flow signal subtracted from the new baseline. This calculation was iterated ten times, and the difference in conversion between iterations was checked to be less than 1×10^{-14}. This calculation was performed for each baseline drawn. Crystallinity was calculated for each thermal event analyzed, using the equation:

$$\mathrm{X_{mc}} = \frac{\Delta \mathrm{H(t)}}{(1 - \mathrm{X_{mr}})\mathrm{H_f^0}} \quad (2)$$

Where $\Delta H(t)$ is the integral of the heat flow curve, normalized for the mass of the sample, X_{mr} is the mass fraction of the fiber reinforcement, $\mathrm{H_f^0}$ is the heat of fusion, and X_{mc} is the mass fraction of crystallinity [2]. The technical datasheet proved the values X_{mr} to be 0.65, and $\mathrm{H_f^0}$ to be 130 J/g [7]. Next, the volume fraction of crystallinity, X_{vc}, was calculated using the equation:

$$\mathrm{X}_{vc} = \frac{\mathrm{X}_{mc}(t)}{\mathrm{X}_{mc}(t) + \frac{\rho_c}{\rho_a}\left(1 - \mathrm{X}_{mc}(t)\right)} \quad (3)$$

Where ρ_c is the density of the crystalline regions of the neat resin (1.365 g/cm^2), and ρ_a is the density of the amorphous regions (1.27 g/cm^2) [2]. These values were also given by the technical datasheet [7].

The cooling crystallization transitions were analyzed for the first cooling cycle of all CF/PEKK experiments. A significant amount of noise in the non-reversing heat flow signals is observed for ramp rates less than 2 °C/min. This noise led to small inconsistencies in the baselines drawn for replicate runs, resulting in a notable difference in the enthalpy of crystallization. Noise is expected for low ramp rates, considering the mass of the resin is only about 1.5 mg. The high ramp rates yielded high-quality signals.

The melting transitions were analyzed by the same method, and specific enthalpy was used to calculate the initial crystallinity before melting. Both the reversing and non-reversing heat flow signals displayed evidence of a melting transition. Despite the careful selection of the modulation parameters to ensure a heat-only MDSC experiment with 5 modulations occurring over the half-height of the transition, the kinetic and thermodynamic components of the crystallization and melting occurring during the melting transition could not be separated (Figure 1). The total heat flow signal was not analyzed although doing so would ensure that the totality of the transition is captured, as the simultaneous melting and crystallization could later be separated [2].

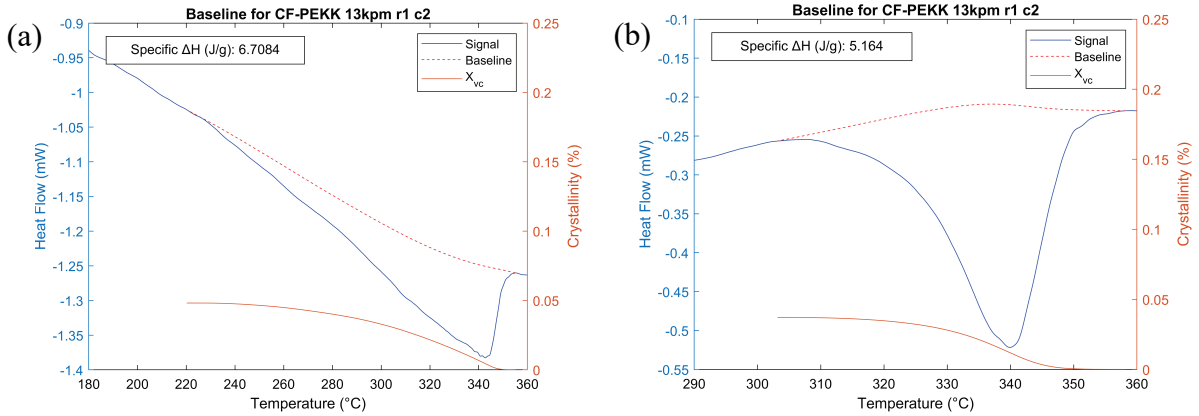

Figure 1. (a) Reversible heat flow vs temperature for melting of CF/PEKK at 13 °C/min during the second heating. Crystallinity as a function of temperature is provided and plotted on a separate axis. (b) Non-reversible heat flow vs temperature for melting of CF/PEKK at 13 °C/min during the second heating. The specific enthalpy of the transitions are listed. The mass of the sample is 5.10 mg, the modulation amplitude ± 0.69 °C, and the modulation period 20 s.

Replicate experiments were analyzed to assess variability. The conversion α signals for each replicate set were interpolated to share common temperatures. The difference in conversion at each temperature was determined, and the root mean square error between the experiments was calculated. The 11 °C/min run showed the lowest error between the replicates. The 1 °C/min run was omitted from the remainder of the analyses due to excessive noise. The 13 °C/min run showed the highest variability, which may be due to equilibrium crystallization occurring at ramp rates below 11 °C/min, according to the manufacturer [7].

Conversion rate dα/dt was plotted against temperature for all ramp rates that were analyzed using the non-reversing heat flow signal (Figure 2). As the ramp rate increases, the maximum rate of conversion also increases. Further, the peak crystallization temperature as well as the two conversion endpoints shift to lower temperatures, and the crystallization temperature range broadens. The melting transitions are also shown on the plot and were constructed using the non-reversing heat flow signals. The peak conversion rate of the melting transitions occurs at roughly

the same temperature regardless of the ramp rate. Additionally, the width of the melting curves appears to remain constant regardless of the ramp rate. These results are consistent with Gordnian's observations while characterizing CF/PEEK [8].

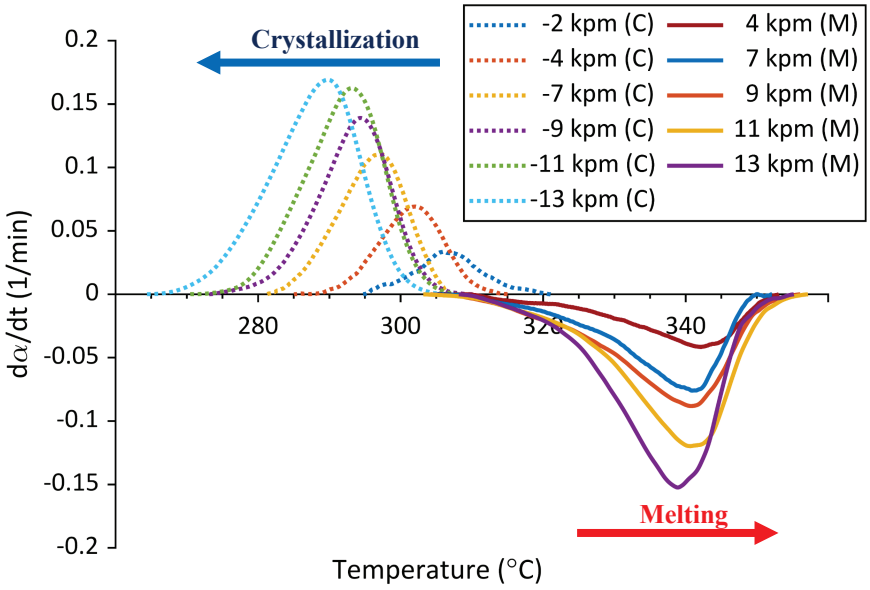

Figure 2. Overlay plot of conversion rate vs temperature for different ramp rates during cooling (C) and melting (M) of CF/PEKK. The melting conversion data were created using the non-reversing heat flow signal.

The reversing heat flow curves were also used to construct baselines for melting transitions. The conversion rates of those analyses are shown in Figure 3, in addition to a select number of cold crystallization analyses and the same set of cooling crystallization analyses. The melting transitions occur over a very broad range, with an onset as low as 200 °C. The cold crystallization events occur between 175 °C and 225 °C, and trend to higher temperatures with higher ramp rates.

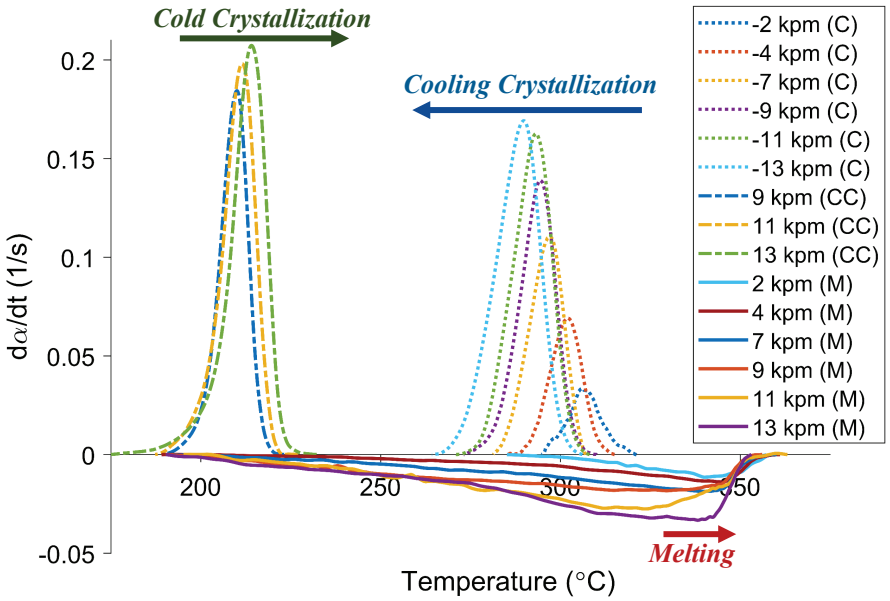

Figure 3. Overlay plot of conversion rate vs temperature for different ramp rates during crystallization (C), cold crystallization (CC) and melting (M) of CF/PEKK. The melting conversion data were created using the reversing heat flow signal.

Unreinforced PEKK was subjected to the same analyses and compared to the results of the CF/PEKK experiments to assess the effect that reinforcement has on the crystallization kinetics. Figure 4 shows the conversion endpoints of PEKK and CF/PEKK at all ramp rates. Both materials show very similar 1% conversion temperatures, although CF/PEKK displays temperatures at 99% conversion which are much higher than PEKK indicating that the increased nucleation sites in CF/PEKK due to the presence of fibers allows for crystallization to occur in smaller temperature range. Both materials show a downward trend in conversion endpoint temperatures with an increasing ramp rate.

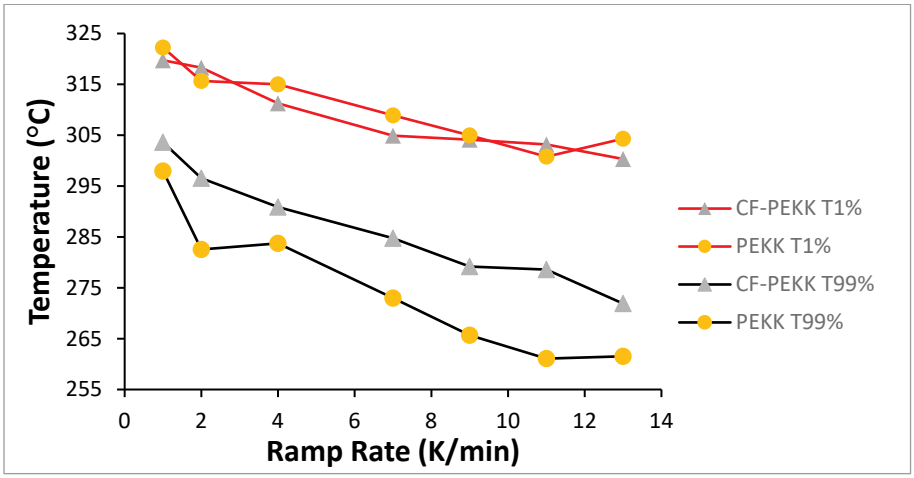

Figure 4. Temperature at 1% and 99% conversion of different ramp rates for CF/PEKK and PEKK, during the first cooling crystallization event.

Crystallinity achieved during cooling crystallization of PEKK and CF/PEKK were measured and compared to literature values available for similar grades of PEKK (Figure 5). The grade of PEKK used in this project is a 70/30 grade, most similar to KEPSTAN® 7003. The KEPSTAN® 6003 shows a trend where crystallinity decreases with ramp rate, although for KEPSTAN® 7003 crystallinity appears to remain constant even at high ramp rates. The measured crystallinity for CF/PEKK shows a significant amount of variability but does not noticeably decrease with ramp rate. PEKK shows less variability, while retaining the same trend of constant crystallinity across ramp rates. The crystallinity of PEKK, even after controlling for the absence of fibers, is higher than CF/PEKK, suggesting that fibers may slightly reduce the degree of crystallinity achieved. The variability in crystallinity for CF/PEKK is attributed to the variation in fiber/resin ratio of the unidirectional tape, since different mass percentages of resin will affect the specific enthalpy of crystallization.

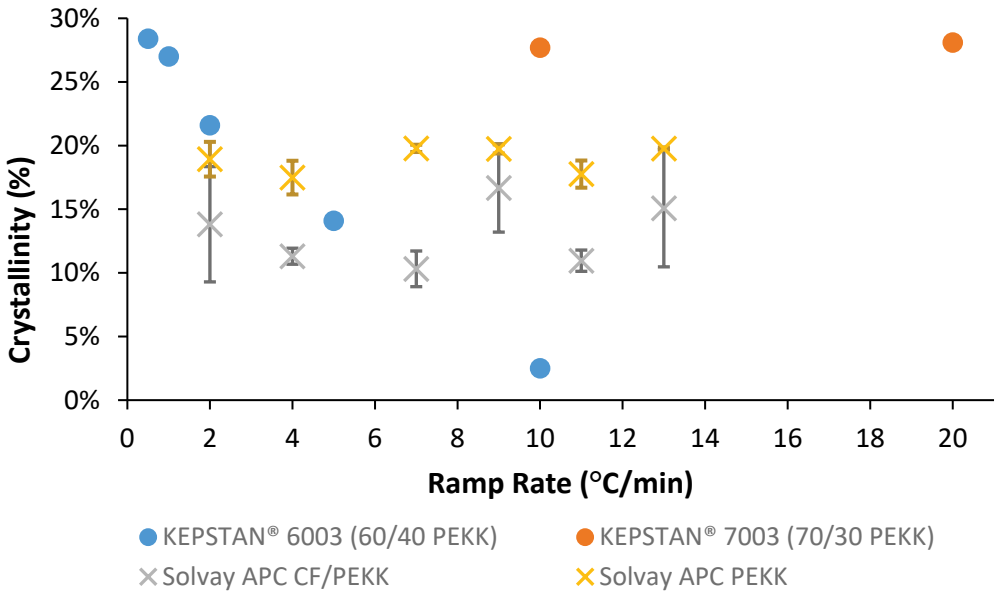

Figure 5. Percent crystallinity vs cooling ramp rate for CF/PEKK, PEKK, and other commercial grades of PEKK (70/30 and 60/40 PEKK) [9]. Error bars represent the sample standard deviation of crystallinity, calculated using the first and second cooling cycles for both replicates.

The first cooling crystallization data for PEKK and CF/PEKK were analyzed by iso-conversional analysis, where the data from the 12 runs for both materials were brought together for 64 different combinatorials. The underlying equations used for this computation are:

$$\Phi(E_\alpha) = \sum_{i=1}^{n} \sum_{j\neq 1}^{n} \frac{I(E_\alpha, T_{\alpha,i})\beta_{j,\alpha}}{I(E_\alpha, T_{\alpha,j})\beta_{i,\alpha}} \quad 4$$

$$I(E_\alpha, T_{\alpha,i}) = \int_{T_{\alpha-\Delta\alpha,i}}^{T_{\alpha,i}} e^{-\frac{E_\alpha}{RT}} dT \quad 5$$

Where α is the extent of conversion, β is the linear temperature ramp rate, E_α is the activation energy, and T is the temperature in °C. Equation 4 is minimized to obtain the result, according to

the methodology outlined by Vyazovkin [10]. This method uses 100 discrete values for α where $\Delta\alpha = 0.01$, while also assuming that E_a is constant over Δα.

CF/PEKK displays a significant amount of variability in E_α, especially for low values of α (Figure 6). PEKK shows noticeably less variability, except for high values of α. The variability in E_α was determined to be a result of variation in fiber/resin ratio of the prepreg. The activation energy for CF/PEKK was calculated to be as low as -309 ± 14.7 kJ/mol for low conversion, while for PEKK it was only found to be as low as -219 ± 3.3 kJ/mol. This indicates that the presence of carbon fibers has a dramatic effect on the crystallization kinetics of CF/PEKK.

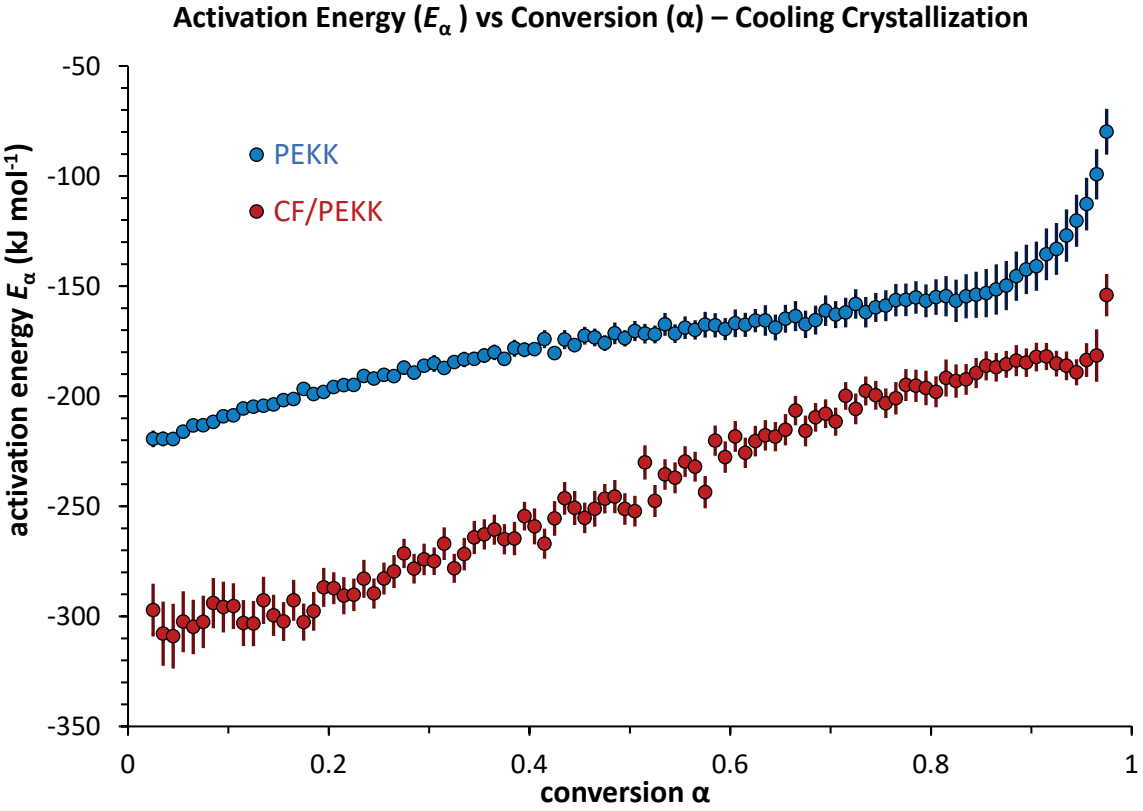

Figure 6. Activation energy (E_α) vs conversion (α), calculated for both neat PEKK and CF/PEKK using the first cooling cycle and both replicates. Error bars represent the 99% confidence intervals of activation energy.

3.2 Isothermal Crystallization Kinetics

Isothermal crystallization kinetics experiments were conducted on CF/PEKK samples to measure the induction time. Drawing the baseline for isothermal crystallization experiments is a known challenge with fast crystallizing materials [8], [11]. Using careful analysis of the temperature and heat flow signals of the experiments, the time between reaching equilibrium and the crystallization peak may be measured. Measuring the enthalpy of these transitions does not provide useful data for the construction of crystallization models. For this analysis, the peak of the crystallization event was considered for calculating induction time, along with the time associated with the local

minimum temperature before crystallization. A clear trend in induction time was observed with increased isothermal crystallization temperature.

3.3 Heat Capacity

Specific heat capacity of PEKK was measured while heating between 50 °C and 250 °C. A sapphire reference sample to calibrate the results [12]. The difference between literature values and the measured specific heat capacity of sapphire is used to create a vertical shift function. This function is then applied to PEKK at specific temperature values to yield the results (Figure 7). Only the thermodynamic, or reversing heat capacity signal from the MDSC experiment should be used for this analysis

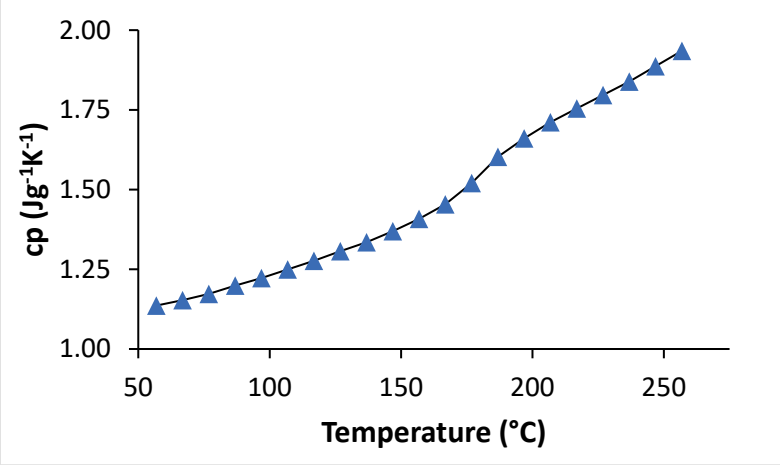

Figure 7. Specific heat capacity vs temperature for CF/PEKK after the calibration.

3.4 Stress Relaxation

Stress relaxation DMA experiments were performed on CF/PEKK samples. The relaxation modulus decreases with increasing temperature (Figure 8), while the largest changes in relaxation modulus are observed at temperatures near the onset of the glass transition (150 °C to 170 °C) and melting (290 °C to 320 °C) [7]. When these same data are plotted with a log scale for relaxation modulus but a linear scale for time, a non-linear decrease in relaxation modulus is observed.

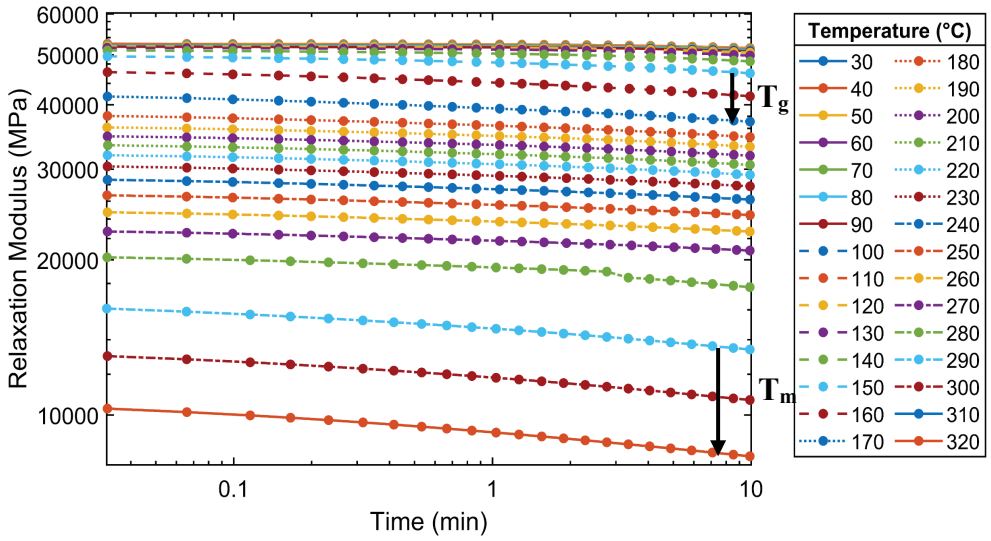

Figure 8. Relaxation modulus vs time of DMA sample 5 for 30 different temperatures. A static strain (0.1%) was applied for 10 minutes at various temperatures between 30 °C and 320 °C.

3.5 Modulus Development

CF/PEKK was subjected to temperature ramp oscillatory DMA experiments using the 3-pt bending fixture. Storage modulus increases slightly from 50 °C to 250 °C, and then drops off dramatically with the approach of the T_g (Figure 9). The peak in tan δ is observed at 171.68 °C, which is nearly 10 °C higher than the T_g listed on TDS for the material [7]. The second peak in tan δ is observed around 225 °C, which may be a pre-melting α transition.

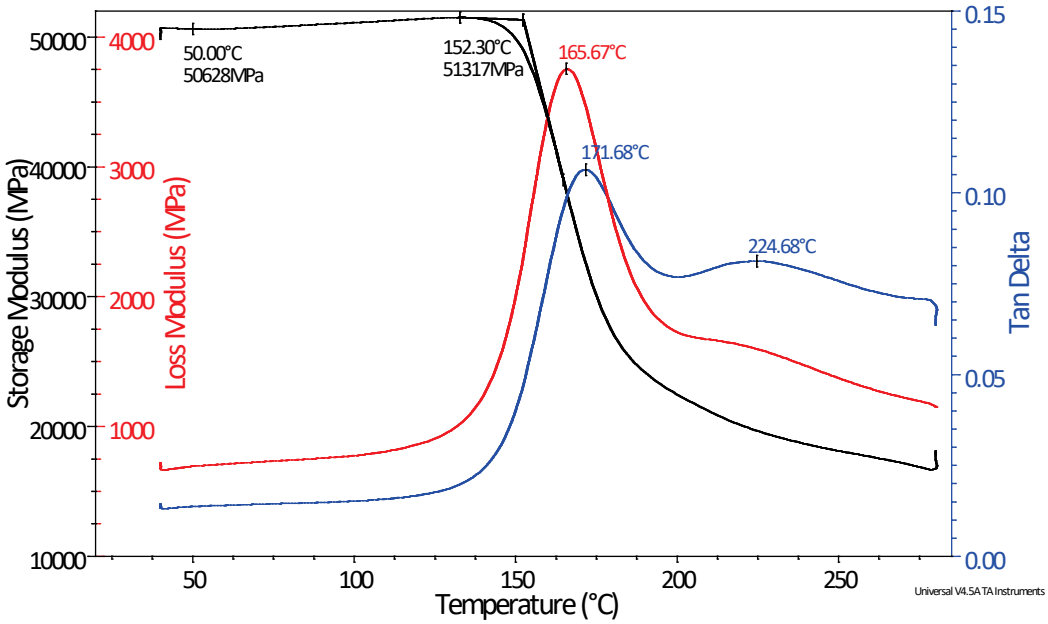

Figure 9. Storage modulus, loss modulus, and tan(δ) vs temperature from DMA dynamic modulus experiment using a 0.1 Hz frequency and 0.1% strain. The modulus at 50 °C and the peaks in tan(δ) are annotated.

3.6 Flow Characteristics

Neat PEKK was characterized by rheology to assess how the viscosity of the material changes over time and temperature. During the cooling cycle, a dramatic increase in complex viscosity is observed near 301 °C, which is consistent with the crystallization temperatures observed with the DSC experiment (Figure 10). There are several abrupt drops in viscosity at lower temperatures, starting at 200 °C, which may be due to slipping of the plates, or a mechanism of crystallization perfection. During the heating cycle, a low-temperature peak in complex viscosity is observed around 235 °C, which is very close to the temperature at which the α transition was observed with the modulus development experiments. Viscosity drops off at 340 °C, just 3 °C higher than the melting temperature of the material cited on the TDS [7].

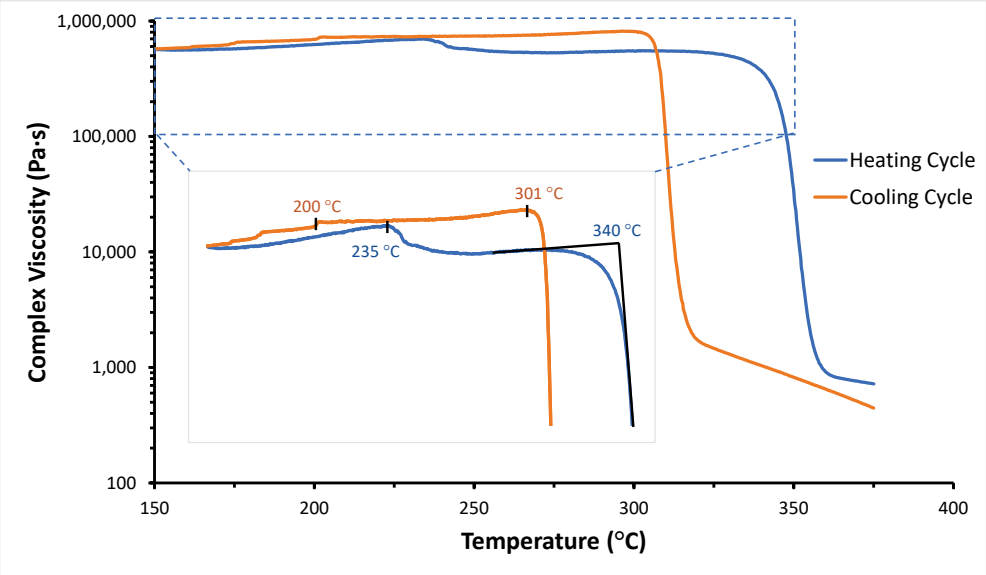

Figure 10. Complex viscosity vs temperature for the neat PEKK rheology experiment performed on sample 2. The strain was held at 0.1% and frequency at 1 Hz as the temperature was ramped from 375-150-375 °C at 2 °C/min.

3.7 Coefficient of Thermal Expansion

The coefficient of thermal expansion was determined using a rheometer. A compressive force of 0.5 N was applied to a sample and applied to the plates without a sample as the temperature was increased from 50 °C to 250 °C. Before performing experiments on the CF/PEKK material, the methodology was first validated using a brass sample (CDA 260) having a known CTE [13]. The gap vs temperature curves for the no-sample calibration run and the sample run was regressed to 5^{th} order polynomials, and the difference between the two polynomials was calculated to yield the true gap vs temperature curve of the sample. The temperature range was narrowed to 75 °C to 225 °C prior to polynomial fitting to eliminate the startup hooks, Finally, this curve was divided by the original measured thickness at 50 °C, to yield an instantaneous CTE curve from which the average linear CTE can be calculated. This methodology applied to the brass calibration sample yielded a result with a 0.3 % difference from the cited value [13]. CF/PEKK was measured using the same methodology to give a CTE of 36.395 μm m^{-1} $°C^{-1}$.

3.8 Density

The density of consolidated CF/PEKK was determined using a DMA bar sample and a density determination kit. Two measurements were taken of the same sample, yielding a density of 1.493 ± 0.035 g/cm^3 at 23.2 °C. A correction factor was applied to ensure that an accurate reference value for the density of air and water was being used, at the ambient temperature during the time of testing. The density was calculated according to the following equation according to Archimedes' principle:

$$\rho = \frac{A}{A - B}(\rho_0 + \rho_L) + \rho_L \qquad 6$$

Where ρ is the density of the sample, A is the weight of the sample in air, B is the weight of the sample in liquid, ρ_0 is the density of the liquid, and ρ_L is the density of air.

3.9 Thermal Conductivity

Thermal conductivity measurements were taken of CF/PEKK after calibrating the instrument with three standard materials. Silicone thermal paste was applied to all samples. The thermal conductivity increases with temperature until the T_g, at which point it decreases slightly (Figure 11). This may be due to the thickness of the sample changing with temperature after the glass transition, affecting the measurement. Variability is observed between the two replicate runs, although this variability is relatively small, and both runs retained the same shape curve. Variability in fiber/resin ratio or in the amount of thermal paste applied may all be causes of this uncertainty.

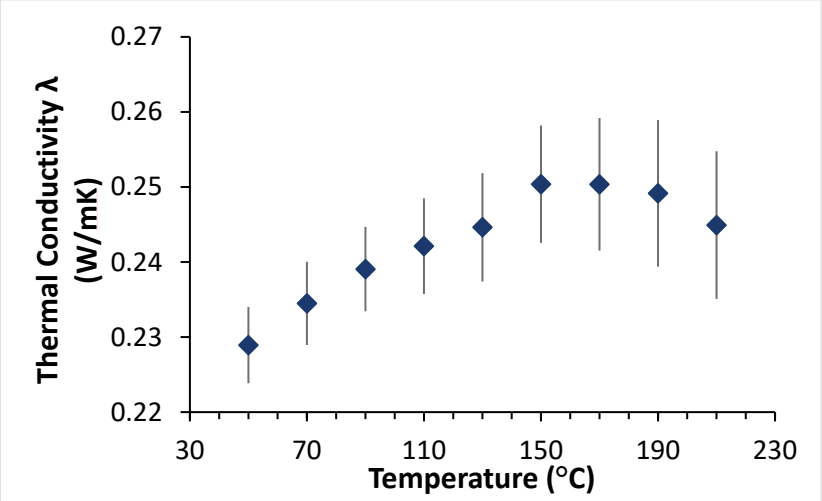

Figure 11. Thermal conductivity vs temperature for CF/PEKK. The error bars represent the range between replicate runs. Tests were conducted in steady-state mode, between 50 °C and 210 °C, and 20 °C intervals.

4. DISCUSSION

4.1 Methods

The crystallization and melting kinetics experimental design yielded high-fidelity data, although specific metrics such as the enthalpy of crystallization and melting did show variability. In Gordnian's 2017 work, only the total heat flow signal was used to study the kinetics [8]. As shown in this work, it is difficult to choose the correct modulation parameters to separate the convoluted thermodynamic and kinetic aspects of the signals, and therefore it may be advantageous to use the total heat flow signal. Even with the uncertainty, the calculated crystallinity did not trend to lower values with higher ramp rates, consistent with the literature for KEPSTAN® 7003 PEKK. The uncertainty is most likely a result of the fiber/resin ratio variation in the unidirectional tape and the difficulties associated with maintaining this ratio when separating a sample from a single ply for analysis. This is supported by the results of the study on unreinforced PEKK, where the variation is considerably diminished. Analysis of the total heat flow signal may reduce the error in the neat PEKK studies to a nominal amount. An additional consideration to be made is the true mass of the resin in the fiber-reinforced samples. A 5 mg CF/PEKK sample would be roughly equivalent to a 1.5 mg sample of PEKK, in terms of the signal-to-noise ratio. This was observed with the 1 °C/min ramp rate experiments, where the signal-to-noise ratio was too low to make use of the data. Therefore, using larger sample masses may also prove advantageous.

A new method was proposed for drawing baselines, wherein the baseline becomes a function of conversion, and may be optimized. This has the effect of reducing user error in drawing the baselines, especially when the heat flow signal appears to approach an asymptote on either side of the thermal event. However, this technique may also result in enthalpies of crystallization of lesser magnitude. Values for the heat of fusion and crystallinity that exist in the literature most likely depend on standard linear baselines, which would skew the results presented in this work.

Thermo-viscoelastic behavior was studied utilizing rheology and DMA experiments. A stress relaxation experimental method was presented, and shown to yield high-fidelity data. Initially, the temperature region between 50 °C and 150 °C was omitted, since the changes in relaxation modulus over this region were expected to be small. However, omitting this temperature region led to poor results, where the relaxation modulus did not show the expected trends with temperature at lower temperatures. The modulus development experiment performed on the DMA yielded reliable data. The rheology temperature ramp experiment also yielded good data. However, the viscosity drops observed at lower temperatures during cooling are yet to be identified as either a true representation of the material's behavior or as an artifact resulting from slipping.

Additional experiments were conducted to determine the CTE, thermal conductivity, and density of the material. Typically, CTE is best determined by thermomechanical analysis (TMA) [14]. In this study, a rheometer was used to measure changes in sample thickness over a range of temperatures. The resulting CTE was not linear, nor could it be modeled by polynomials with favorable residual patterns. Following the ASTM standard test method or using fractional polynomial models would be recommended. Thermal conductivity measurements yielded good data, although factors such as the amount of thermal paste applied or the fiber/resin ratio of the samples should be accounted for in future work. Density measurements were consistent, although the deviation from the expected value further highlighted the importance of accounting for fiber/resin ratios in samples.

4.2 Material Behavior

Crystallization and melting kinetics studies revealed that the presence of fiber both increases the magnitude of the activation energy E_α, while also increasing the rate of crystallization, likely through increased nucleation sites. However, fiber reinforcement may reduce the maximum achievable degree of crystallinity. An inaccurate fiber/resin ratio would also yield the same result, however. CF/PEKK did not show signs of secondary crystallization; the study on PEKK did show signs of secondary crystallization though only at the highest ramp rate.

The results of the stress relaxation experiment show that the relaxation modulus decreases with increasing temperature, however, this decrease in modulus is most dramatic over temperatures near the onset of T_g and T_m. An Arrhenius relationship between relaxation modulus and time was not observed. The modulus development experiment suggested a T_g of 171.68 °C. Interestingly, a second $\tan(\delta)$ peak was observed after the T_g, near 225 °C. A similar observation was made in the viscosity rheology experiments, where a pre-melting peak in complex viscosity occurred at 235 °C. These peaks may both be suggesting a characteristic α-relaxation transition before melting.

5. CONCLUSIONS

CF/PEKK unidirectional tape prepreg was studied, and its material behavior was characterized. Studies were performed to investigate crystallization and melting kinetics, specific heat capacity, stress relaxation, modulus development, viscosity, CTE, thermal conductivity, and density characteristics and properties. The data was collected and presented to prepare for model fitting and the construction of constitutive equations that may be used with process models. The potential issues with the experiments or analyses were identified and brought to the attention of the reader. Recommended changes to experimental conditions were described along with the rationale for doing so. Observations of the material's behavior were described concerning the crystallization kinetics, stress relaxation behavior, and viscosity and modulus development characteristics. This work serves as a framework for other scientists and engineers with the goals to fully characterize a thermoplastic prepreg composite material, for the construction of process models.

6. REFERENCES

[1] N. Zobeiry *et al.*, "Multiscale characterization and representation of composite materials during processing," *Phil. Trans. R. Soc. A.*, vol. 374, no. 2071, p. 20150278, Jul. 2016, doi: 10.1098/rsta.2015.0278.

[2] K. Gordnian, "Crystallization and thermo-viscoelastic modelling of polymer composites," University of British Columbia, 2017. doi: 10.14288/1.0357195.

[3] J. Teltschik, D. Fricke, and M. Horn, "Efficient Determination of Material Parameters for Robust Process Simulation of Semi-Crystalline Thermoplastic Composites," presented at the ITHEC 2020, Bremen, Deutschland, Oct. 2020. Accessed: Nov. 02, 2021. [Online]. Available: https://elib.dlr.de/138378/

[4] M. Barile, L. Lecce, M. Iannone, S. Pappadà, and P. Roberti, "Thermoplastic Composites for Aerospace Applications," in *Revolutionizing Aircraft Materials and Processes*, S. Pantelakis and K. Tserpes, Eds. Cham: Springer International Publishing, 2020, pp. 87–114. doi: 10.1007/978-3-030-35346-9_4.

[5] A. J. Comer *et al.*, “Mechanical characterisation of carbon fibre–PEEK manufactured by laser-assisted automated-tape-placement and autoclave,” *Composites Part A: Applied Science and Manufacturing*, vol. 69, pp. 10–20, Feb. 2015, doi: 10.1016/j.compositesa.2014.10.003.

[6] P. G. Guest and P. G. Guest, *Numerical Methods of Curve Fitting*. Cambridge University Press, 2012. [Online]. Available: https://books.google.com/books?id=UjnB0FIWv_AC

[7] “Solvay APC (PEKK) Thermoplastic composite tapes,” *Solvay*. https://www.solvay.com/en/product/apc-pekk-thermoplastic-composite-tapes (accessed Nov. 04, 2021).

[8] K. Gordnian, “Crystallization and thermo-viscoelastic modelling of polymer composites,” 2017, doi: 10.14288/1.0357195.

[9] L. Quiroga Cortés, N. Caussé, E. Dantras, A. Lonjon, and C. Lacabanne, “Morphology and dynamical mechanical properties of poly ether ketone ketone (PEKK) with meta phenyl links,” *J. Appl. Polym. Sci.*, vol. 133, no. 19, p. n/a-n/a, May 2016, doi: 10.1002/app.43396.

[10] *Isoconversional Kinetics of Thermally Stimulated Processes*. Accessed: Jun. 04, 2022. [Online]. Available: http://link.springer.com/book/10.1007/978-3-319-14175-6

[11] T. Choupin, B. Fayolle, G. Régnier, C. Paris, J. Cinquin, and B. Brulé, “Isothermal crystallization kinetic modeling of poly(etherketoneketone) (PEKK) copolymer,” *Polymer*, vol. 111, pp. 73–82, Feb. 2017, doi: 10.1016/j.polymer.2017.01.033.

[12] L. T. Sin, W. A. W. A. Rahman, A. R. Rahmat, N. A. Morad, and M. S. N. Salleh, “A Study of Specific Heat Capacity Functions of Polyvinyl Alcohol–Cassava Starch Blends,” *Int J Thermophys*, vol. 31, no. 3, pp. 525–534, Mar. 2010, doi: 10.1007/s10765-010-0744-6.

[13] J. R. Davis and ASM International, Eds., *Copper and copper alloys*. Materials Park, OH: ASM International, 2001.

[14] “Standard Test Method for Linear Thermal Expansion of Solid Materials by Thermomechanical Analysis.” https://www.astm.org/e0831-19.html (accessed Jun. 12, 2022).